Impacts of the Silk Road pattern on the interdecadal variations of the atmospheric heat source over the Tibetan Plateau

Han, Yizhe ; Ma, Weiqiang; Yang, Yaoxian ; Ma, Yaoming; Xie, Zhipeng ; Sun, Genhou; Menenti, Massimo; Su, Bob

DOI
10.1016/j.atmosres.2021.105696

Publication date
2021

Document Version
Final published version

Published in
Atmospheric Research

Citation (APA)
Han, Y., Ma, W., Yang, Y., Ma, Y., Xie, Z., Sun, G., Menenti, M., & Su, B. (2021). Impacts of the Silk Road pattern on the interdecadal variations of the atmospheric heat source over the Tibetan Plateau. *Atmospheric Research*, *260*, 1-14. Article 105696. https://doi.org/10.1016/j.atmosres.2021.105696

Atmospheric Research 260 (2021) 105696

Contents lists available at ScienceDirect

Atmospheric Research

journal homepage: www.elsevier.com/locate/atmosres

Impacts of the Silk Road pattern on the interdecadal variations of the atmospheric heat source over the Tibetan Plateau

Yizhe Han [a,b], Weiqiang Ma [a,b,*], Yaoxian Yang [c,**], Yaoming Ma [a,b,d], Zhipeng Xie [a], Genhou Sun [e,f], Massimo Menenti [g,h], Bob Su [i,j]

[a] Key Laboratory of Tibetan Environment Changes and Land Surface Processes, Institute of Tibetan Plateau Research, Chinese Academy of Sciences, Beijing 100101, China
[b] University of Chinese Academy of Sciences, Beijing 100049, China
[c] Key Laboratory for Land Process and Climate Change in Cold and Arid Regions, Northwest Institute of Eco-Environment and Resources, Chinese Academy of Science, Lanzhou 730000, China
[d] CAS Center for Excellence in Tibetan Plateau Earth Sciences, Beijing 100101, China
[e] Key Laboratory for Climate Change and Natural Disaster Studies, School of Atmospheric Sciences, Sun Yat-Sen University, Guangzhou 510275, China
[f] Southern Marine Science and Engineering Guangdong Laboratory, Zhuhai 519082, China
[g] State Key Laboratory of Remote Sensing Science, Institute of Remote Sensing and Digital Earth, Chinese Academy of Sciences, Beijing 100101, China
[h] Delft University of Technology, 2628, CN, Delft, the Netherlands
[i] Faculty of Geo-Information Science and Earth Observation, University of Twente, Enschede 7500AE, the Netherlands
[j] Key Laboratory of Subsurface Hydrology and Ecological Effect in Arid Region of Ministry of Education, School of Water and Environment, Chang'an University, Xi'an 710054, China

ARTICLE INFO

Keywords:
Tibetan Plateau
Reanalysis datasets
Silk Road Pattern (SRP)
Atmospheric heat source
Interdecadal variability

ABSTRACT

This study aimed to investigate the relationship between the boreal summer Silk Road Pattern (SRP) and the atmospheric heat (<Q1>) over the Tibetan Plateau (TP) region, using 5 reanalysis datasets over the period 1979–2019. Our results indicate an interdecadal change of boreal summer SRP over the Eurasian region, with a regime shift in the spatial structure at around 1997. Meanwhile, the summer <Q1> anomaly also shows a clear interdecadal increasing trend over the TP region, which is highly correlated with the interdecadal variation of the SRP. The impact of the SRP on the summer <Q1> was also investigated. The regime shift of the SRP would have generated circulation anomalies over the Lake Baikal region in 500 hPa, which would have inhibited moisture transport across the eastern boundary of the TP. Meanwhile, Indian Summer Monsoon (ISM) would also transport water vapor through the southern boundary of the TP and increased the contents of water vapor in the TP. Associated with this increase in moisture, the change of vertical motion would result in large plenty of precipitation, which released latent heat and enhanced <Q1> in summer. Thus, the regime shift in summer SRP was an important factor contributing to changes in summer <Q1> over the TP in recent decades.

1. Introduction

The Tibetan Plateau (TP) is the world's largest plateau, and is regarded as the "Third Pole". The TP is characterized by complex topography and surface conditions (Qiu, 2008), and as a significant heat source, the TP not only has a great impact on the Asian Summer Monsoon (ASM) (Yanai et al., 1992; Yanai and Li, 1994; Li and Yanai, 1996) but also plays an important role in the weather systems of China (Tao and Ding, 1981; Hsu and Liu, 2003; Chen et al., 2015) and climate patterns of East Asia (Li and Yanai, 1996). Meanwhile, due to the TP's unique geographical location and high elevation, climate change has had a greater impact on the TP than on the surrounding regions (Liu and Chen, 2000; Zhu et al., 2001; Niu et al., 2004; Qin et al., 2009). In this climate context, a much better understanding of the characteristics of

* Corresponding author at: Key Laboratory of Tibetan Environment Changes and Land Surface Processes, Institute of Tibetan Plateau Research, Chinese Academy of Sciences, Beijing 100101, China.
** Corresponding author at: Key Laboratory for Land Process and Climate Change in Cold and Arid Regions, Northwest Institute of Eco-Environment and Resources, Chinese Academy of Science, Lanzhou 730000, China.
E-mail addresses: wqma@itpcas.ac.cn (W. Ma), yangyaoxian@nieer.ac.cn (Y. Yang).

https://doi.org/10.1016/j.atmosres.2021.105696
Received 10 October 2020; Received in revised form 2 February 2021; Accepted 22 May 2021
Available online 26 May 2021

variations in the region's atmospheric heat sources (<Q1>) is needed. Many studies have investigated the characteristics of <Q1> over the TP (e.g. Luo and Yanai, 1984; Wu et al., 2015; Duan and Wu, 2005; Zhu et al., 2012; Shi and Liang, 2014; Chen et al., 2015); for example, <Q1> over the TP has been recognized as one of the most important factors modulating the onset and intensity of the Asian Summer Monsoon (ASM) (e.g. Zhao and Chen, 2001; Wu et al., 2007, 2015). The interdecadal variations in <Q1> have also been analyzed (Jiang et al., 2016; Xie and Wang, 2019; Han et al., 2019), along with the mechanisms responsible for variations in <Q1> over the TP. For example, Qian et al. (2003) found that snow cover could alter <Q1> over the TP, Zhu et al. (2007) indicated that the long-term interaction between moist soil and the atmosphere can influence <Q1> over the TP, and Cui et al. (2015) analyzed the relationship between spring <Q1> and North Atlantic sea surface temperature anomalies (SSTAs). Zhao et al. (2018) illustrated that Indian ocean forcing would also affect the variation of <Q1> over the TP, and Ren et al. (2019) argued that quasi-biweekly variability of the South Asian high would affect <Q1> during summer. Furthermore, snow depth has also been shown to influence <Q1> of the TP (Xiao et al., 2019). In 2019, Lu et al. (2019) found that variations in Atlantic SST could affect <Q1> of the TP, but the mechanism still needs to be further investigated.

The Silk Road Pattern (SRP) is an obvious zonally-oriented teleconnection pattern in the boreal summer over Eurasia. Analyses of the SRP by Lu et al. (2002) and Enomoto et al. (2003) confirmed that this pattern represents a stationary Rossby wave trapped in the jet stream, with several geographically fixed centers. These centers are distributed from northwestern Africa to East Asia (Lu et al., 2002; Enomoto et al., 2003). With a broad extent from Europe to East Asia, the SRP exerts a strong influence on the climate of these regions; for example, the precipitation and surface air temperature (e.g. Lu et al., 2002; Enomoto et al., 2003; Enomoto, 2004; Ding and Wang, 2005; Huang et al., 2011; Su and Lu, 2014; Hong and Lu, 2016; Hong et al., 2017). The corresponding wave index is defined as the first-mode principal component of the empirical orthogonal function (EOF) decomposition for the meridional wind anomaly (including spatial and temporal patterns) at 200 hPa (V200) over the Eurasian region of 20° to 60°N, 0° to 150°E (Yasui and Watanabe, 2010). At present, there are still some controversies about the formation mechanism of the SRP. Some scholars have suggested that the SRP is an internal atmospheric mode because the spatial structure of the SRP can be well reproduced in a dry atmosphere model driven by time-varying or long-term mean diabatic heat (Yasui and Watanabe, 2010). Some scholars thought that external atmospheric forcing also plays an important role in the formation of the SRP (Yasui and Watanabe, 2010; Ding and Wang, 2005; Chen and Huang, 2012; Ding et al., 2011). For instance, the diabatic heating over the Indian summer monsoon region or the Indian Ocean could excite and modulate the phases of the SRP (Ding et al., 2011; Chen and Huang, 2012). The El Niño–Southern Oscillation (ENSO) has also been demonstrated to have an impact on the SRP (Ding et al., 2011). However, the relationship between the SRP and these external atmospheric factors could be unstable (Kosaka et al., 2012; Wang et al., 2012). For instance, since the influences of ENSO on the Asian monsoon is time-varying and depends on the decadal oceanic variability such as the Pacific Decadal Oscillation (Kumar et al., 1999; Chen et al., 2013; Feng et al., 2014). This time-varying feature may influence the relationship between ENSO and the SRP.

It should be emphasized that former studies focus on the interannual timescale, the interdecadal characteristics of the SRP have also received much attention. For example, many studies have considered interdecadal changes of the SRP and of climatic phenomena associated with changes in the SRP (Hong and Lu, 2016; Kosaka et al., 2009; Sato and Takahashi, 2006; Song et al., 2013; Piao et al., 2017; Chen and Huang, 2012; Wu et al., 2016). Wang et al. (2017) analyzed the interdecadal features of the SRP and found that the SRP index experiences two regime shifts, in 1972 and 1997. Also, they illustrated that the Atlantic Multidecadal Oscillation is a plausible driver of the SRP. Chowdary et al. (2019) illustrated that the SRP which embedded in the Asian jet in association with western North Pacific circulation and the Pacific-Japan pattern would alter the strength and phase of the monsoon. Hong et al. (2018) compared the interdecadal and interannual characteristics of the SRP, finding that the decadal SRP is similar to the interannual SRP from Europe to Central Asia, but has a weak meridional wind anomaly over East Asia. Hong et al. (2017) found that the structure of the SRP in Europe, West Asia and Northeast Asia has undergone obvious changes with the intensification of summer warming. Piao et al. (2017) illustrated that the change of the SRP after the late 1990s would have led to a decrease in summer precipitation over the Asian inland plateau region.

Table 1
Locations and characteristics of the study sites in the TP.

Site	Latitude	Longitude	Altitude	Periods of radiosonde data
QOMS	28.21	86.56	4276	14th to 18th of May 2019; 27th July to the 2nd of August 2019
SETORS	29.46	94.44	3326	14th to 18th of May 2019; 27th July to the 2nd of August 2019
NPCE	31.37	91.90	4509	14th to 18th of May 2019; 27th July to the 2nd of August 2019
NADORS	33.39	79.70	4270	14th to 18th of May 2019; 27th July to the 2nd of August 2019

There are many studies on the long-term changes in the SRP and <Q1> over the TP in boreal summer, and the impact of these changes on the climate over the northern hemisphere. Previous studies tend to separate the SRP and <Q1>, and rarely analyzed the relationships between them. Besides, both are important factors influencing the atmospheric circulation system in the northern hemisphere in summer, but it is unclear whether there is a correlation between the variations in the SRP and <Q1>. To better understand the relationship between the SRP and <Q1>, three questions need to be answered. Firstly, is there a relationship between the SRP (a large-scale atmospheric system spanning Eurasia) and <Q1> of the TP? Secondly, does the long-term variation in the SRP affect the variation of summer <Q1> over the TP? Thirdly, if there is an impact, what is the mechanism? To answer those questions, the present study examines the relationship between the long-term variation in the summer SRP and <Q1> over the TP, and assesses the associated physical processes.

The remainder of this paper is organized as follows. In section 2, we provide a brief overview of the datasets, methods and calculations we used in this study. In section 3, we verify the accuracy of the ERA-Interim high-level reanalysis data (ERA-Interim data) by radiosonde data. In section 4, we investigate the relationship between the SRP and <Q1> over the TP. An associated physical explanation will follow in section 5, and we offer conclusions in section 6.

2. Data and method

We used the daily European Centre for Medium-Range Weather Forecasts Interim reanalysis (ERA-Interim; Dee et al., 2011) and ERA-5 data (Hersbach et al., 2019) with a horizontal resolution of 1.5° (latitude and longitude) over the period 1979–2019. Besides, the reanalysis data from National Centers for Environmental Predictions(NCEP)/Department of Energy (DOE) (NCEP-DOE; Kanamitsu et al., 2002), The modern-era retrospective analysis for research and applications version 2 (MERRA-2; Gelaro et al., 2017) and the Japanese 55-year Reanalysis data (JRA-55) (Kobayashi et al., 2015) are also used to calculate the summer <Q1> in the TP. The temperature, zonal wind, meridional wind, and vertical velocity extracted from those 5 reanalysis data from 1000 hPa to 100 hPa are used to calculate <Q1> over the TP. Also, the geopotential height is used to depict the Rossby wave train (RWT) pattern of the SRP over the mid-latitude and subtropical regions.

The radiosonde observational data were collected at the Ngari Station for Desert Environment Observation and Research (NADORS), the Naqu Station of Plateau Climate and Environment (NPEC), the

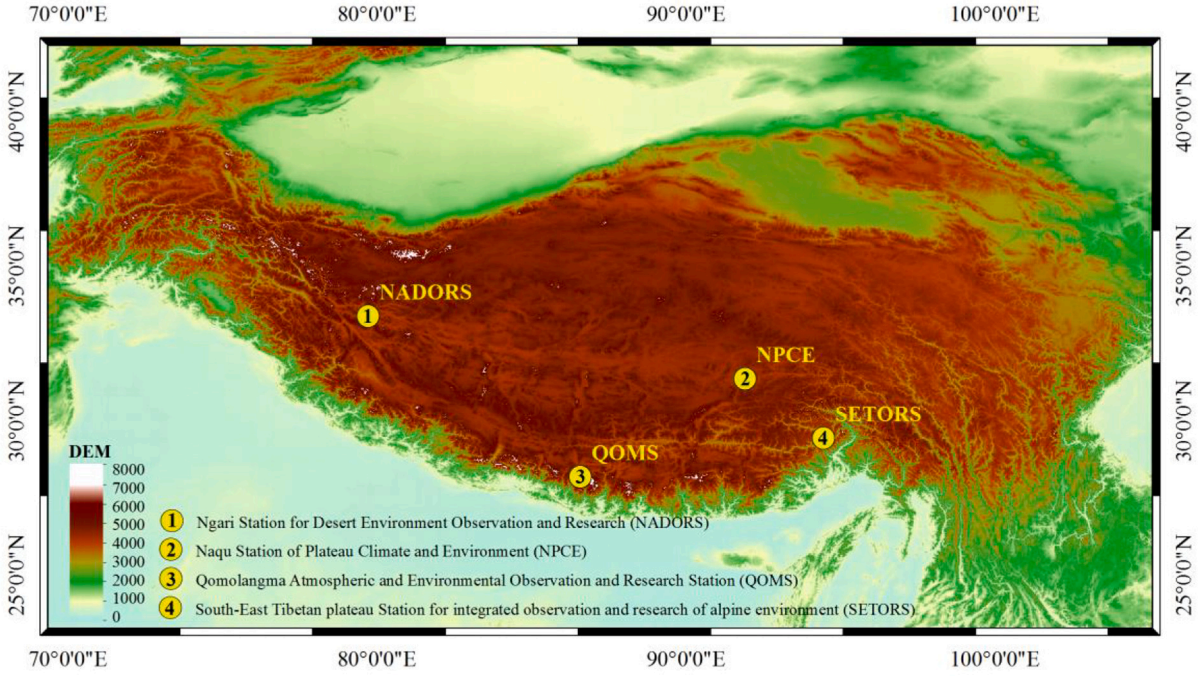

Fig. 1. The terrain of the Tibetan Plateau (TP). Altitude is shown in the color bar (m ASL).
(1) Ngari Station for Desert Environment Observation and Research (NADORS).
(2) Naqu Station of Plateau Climate and Environment (NPEC).
(3) Qomolangma Atmospheric and Environmental Observation and Research Station (QOMS).
(4) South-East Tibetan Plateau Station for integrated Observation and Research of Alpine Environments (SETORS).

Qomolangma Atmospheric and Environmental Observation and Research Station (QOMS), and the South-East Tibetan Plateau Station for Integrated Observation and Research of Alpine Environments (SETORS). We used these data to verify the high-level data collected from 5 reanalysis data. The characteristics of those four sites can be found in Table 1 and Fig. 1. The radiosonde observations are made at 0000 UTC (0800 Chinese standard time (CST)), 0600 UTC (1400 CST), 1200 UTC (2000 CST) and 1800 UTC (0200 CST). These observations

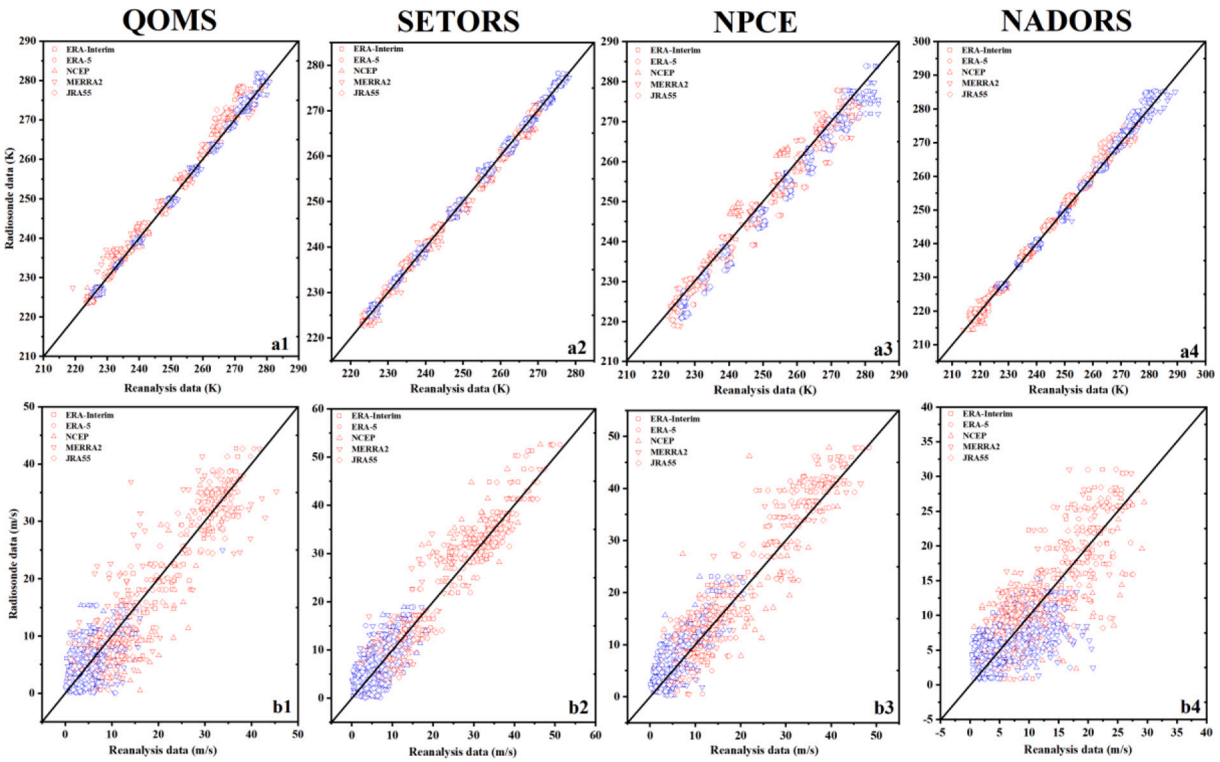

Fig. 2. Scatter plot for different reanalysis data and radiosonde data of (a) air temperature, (b) wind speed. The red scatters represent the data from 14th to 18th of May 2019. The blue scatters represent the data from 27th July to the 2nd of August 2019.

Table 2
The RMSEs and Correlation coefficients for air temperature between radiosonde data and different reanalysis datasets in 4 sites.

	ERA-Interim	ERA-5	NCEP-DOE	MERRA2	JRA-55
RMSEs (QOMS)	1.66	1.56	1.85	1.82	1.79
RMSEs (SETORS)	0.79	0.74	1.26	1.1	0.84
RMSEs (NPCE)	3.14	3.01	3.95	3.47	2.96
RMSEs (NADORS)	1.17	1.15	1.66	1.54	1.98
RMSEs (average)	1.69	1.61	2.18	1.98	1.89
Correlation coefficients (QOMS)	0.996**	0.997**	0.994**	0.994**	0.996**
Correlation coefficients (SETORS)	0.999**	0.999**	0.997**	0.998**	0.999**
Correlation coefficients (NPCE)	0.990**	0.991**	0.967**	0.988**	0.990**
Correlation coefficients (NADORS)	0.998**	0.998**	0.998**	0.997**	0.997**
Correlation coefficients (average)	0.995**	0.996**	0.989**	0.994**	0.995**

*: 95%significance test. **:99% significance test.

Table 3
The RMSEs and correlation coefficients for wind speed between radiosonde data and different reanalysis datasets in 4 sites.

	ERA-Interim	ERA-5	NCEP-DOE	MERRA2	JRA-55
RMSEs (OMS)	3.26	2.96	5.28	5.77	3.65
RMSEs (SETORS)	3.20	2.80	4.31	3.65	3.16
RMSEs (NPCE)	3.58	3.75	5.61	3.60	3.88
RMSEs (NADORS)	3.32	2.97	4.91	4.72	4.01
RMSEs (average)	3.34	3.12	5.02	4.43	3.67
Correlation coefficients (QOMS)	0.958**	0.966**	0.857**	0.828**	0.947**
Correlation coefficients (SETORS)	0.965**	0.973**	0.943**	0.944**	0.964**
Correlation coefficients (NPCE)	0.959**	0.953**	0.896**	0.942**	0.958**
Correlation coefficients (NADORS)	0.850**	0.881**	0.676**	0.652**	0.766**
Correlation coefficients (average)	0.933**	0.943**	0.843**	0.841**	0.908**

*: 95%significance test. **:99% significance test.

are carried out only in fine weather to ensure the accuracy of the data. We selected and compared two types of data for the same periods and heights to enable comparison of the reanalysis data and radiosonde data.

<Q1> is calculated according to Luo and Yanai (1984):

$$Q_1 = C_P\left[\frac{\partial T}{\partial t} + \overline{V}\cdot\nabla T + \left(\frac{p}{p_0}\right)^K \omega\frac{\partial\theta}{\partial p}\right] \quad (1)$$

$$< Q_1 >= \frac{1}{g}\int_{P_t}^{P_S} Q_1 dp \approx LP + Q_S + < Q_R > \quad (2)$$

Q_1 is the atmospheric heat source, T is atmospheric temperature, V is wind velocity for the zonal and meridional components, respectively (U-wind and V-wind), θ is the potential temperature, p is pressure, and ω is vertical velocity. $K = R/C_p$; C_p is the specific heat at a constant pressure of dry air and R is the gas constant. P_s refers to surface pressure and P_t = 100 hPa. L is latent heat due to condensation, P is the precipitation rate, Q_s is surface sensible heat flux and $<Q_R>$ is the radiative heating (cooling) rate. Vertical integration is represented by <>. In the present study, we calculated <Q1> from every 6 hourly sets of measurements, then averaged across different seasons to ensure the accuracy of the conclusion. Besides, the water vapor flux (Q2) at 500 hPa is utilized to analyze variations of water vapor over the TP:

$$Q2 = -\frac{1}{g}(q^*V) \quad (3)$$

Q2 is the water vapor flux, q is specific humidity.

We also carried out regression analyses to look for a relationship between two variables, and we assessed these analyses using the Student *t*-test. We used the Mann-Kendell test (MK-Test) to analyze trends and to detect abrupt change points.

3. Verification of 5 different reanalysis data

There are few meteorological observation sites on the TP due to the high altitude and harsh natural environment. Most of these sites are concentrated in the central-eastern TP and located below 5000 m above sea level (ASL) (Duan et al., 2014). Thus, it is difficult to use observational data to analyze the climatic features of the TP, and most studies in this area have required reanalysis data. Furthermore, as there are no routine quantitative observations of the atmosphere, reanalysis data is the only way to calculate <Q1>. For these reasons, we have verified 5 reanalysis datasets in the present study.

According to Luo and Yanai (1984), <Q1> can be calculated using temperature, wind velocity and vertical velocity in the atmosphere (i.e. by Eq. 1). Here we compare the temperature and wind speed from radiosonde data collected at QOMS, SETORS, NPCE and NADORS with ERA-Interim data, ERA-5 data, NCEP-DOE data, MERRA2 data and JRA-55 data between 550 hPa and 200 hPa to verify their accuracy.

We compare the temperature and wind speed of the 5 reanalysis datasets and radiosonde data at these 4 sites during May and July 2019 (Fig. 2). The root means square errors (RMSEs) and correlation coefficients between the reanalysis data and radiosonde data are shown in Tables 2 and 3. The conclusion illustrates that there is a good correlation between air temperature of the reanalysis datasets and radiosonde data; almost all correlation coefficients exceed 0.99 and pass the 99% significance test, indicating good consistency between the observation data and reanalysis data. The temperature RMSEs for those 5 reanalysis datasets are around 2 °C, indicating small errors of those reanalysis datasets. The correlation coefficients for the wind speed of the 5 reanalysis datasets are lower than those for air temperature. Meanwhile, the RMSEs for wind speed are larger than that for air temperature. However, all correlation coefficients for wind speed exceed 0.84 and pass the 99% significance test, indicating those reanalysis datasets have good correlations and consistency. The RMSEs of the wind speed ranging from 3.1 °C to 5.0 °C, which indicates better performance of ERA-5 and ERA-Interim data. Another point worth noting is that the 5 reanalysis datasets have obvious differences at different sites. The temperature RMSEs of the 5 reanalysis data in NPCE is larger than other sites, while the RMSE of wind speed does not have obvious site differences.

In general, ERA-5 data showed the best performance at the 4 sites, with the smallest bias and the highest correlation coefficients compared with the observation data, followed by the ERA-Interim data and JRA-55 data. The MERRA2 and NCEP-DOE data, however, shows larger bias and lower correlation coefficients, especially for the wind speed. Our verification indicated that ERA-5 data have a smaller bias, better applicability, and higher accuracy in the TP. Therefore, the ERA-5 data are the most suitable data for studying the atmospheric characteristics of the TP.

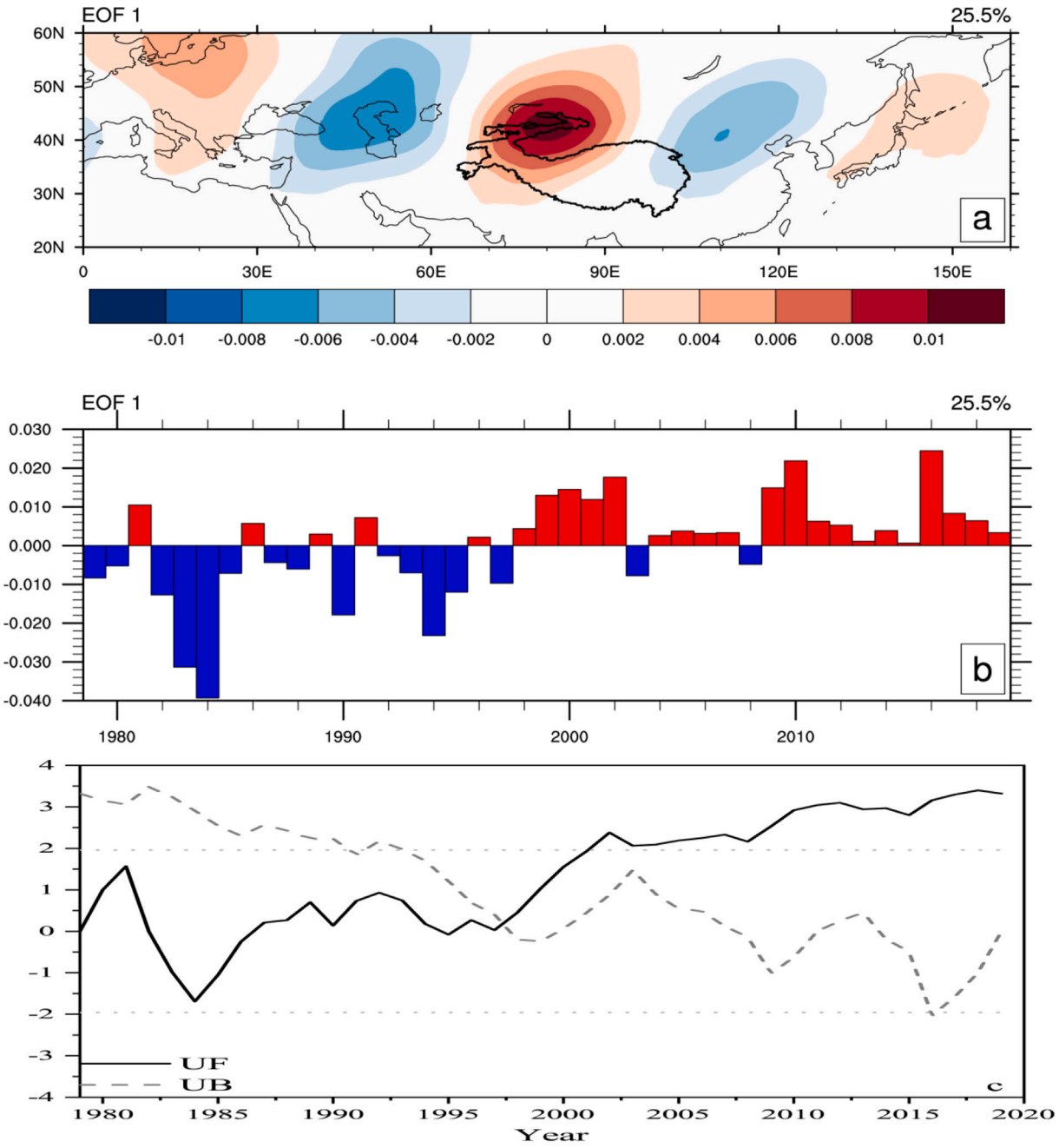

Fig. 3. EOF of V-wind at 200 hPa (a, b) and the MK-Test of the temporal pattern (c).
(a) The spatial pattern of V-wind at 200 hPa over Eurasia. The colored areas indicate the high (low) value areas of V-wind in 200 hPa. The black line indicates the TP region.
(b) Temporal pattern of V-wind at 200 hPa over Eurasia. The colored bars show the time series of V-wind at 200 hPa.
(c) MK-Test of the temporal pattern of V-wind at 200 hPa over Eurasia.
MK-Test of time series of V-wind at 200 hPa. The black curve is the UF line and the gray dotted line is the UB line; the ordinate is the 0.05 significance level and the critical value of this level. The intersection of the UF and UB lines is the abrupt change point.

4. Relationship between interdecadal variability of the SRP and <Q1> in the TP region during the boreal summer

4.1. Variations of the SRP in the boreal summer

Previous studies have shown that the SRP is a stationary Rossby wave train (RWT) trapped in the subtropical Asian westerly jet stream (Lu et al., 2002; Enomoto et al., 2003). Other previous studies analyzed the long-term variation characteristics of the SRP (Wang et al., 2017; Hong et al., 2018). However, most of those studies select the National Centers for Environmental Prediction (NCEP)-National Center for Atmospheric Research (NCAR) reanalysis dataset and JRA-55 data for analysis due to their longer time series. In this study, we selected the ERA-5 data to further analyze the characteristics of the summer <Q1> over the TP because we have verified the accuracy of these data for the TP region. To eliminate the errors associated with using multiple different datasets, and to ensure the accuracy of the results, we used the ERA-5 data to analyze the SRP even though this dataset is not available for as long a duration as other datasets.

According to the definition of SRP wave index (Yasui and Watanabe,

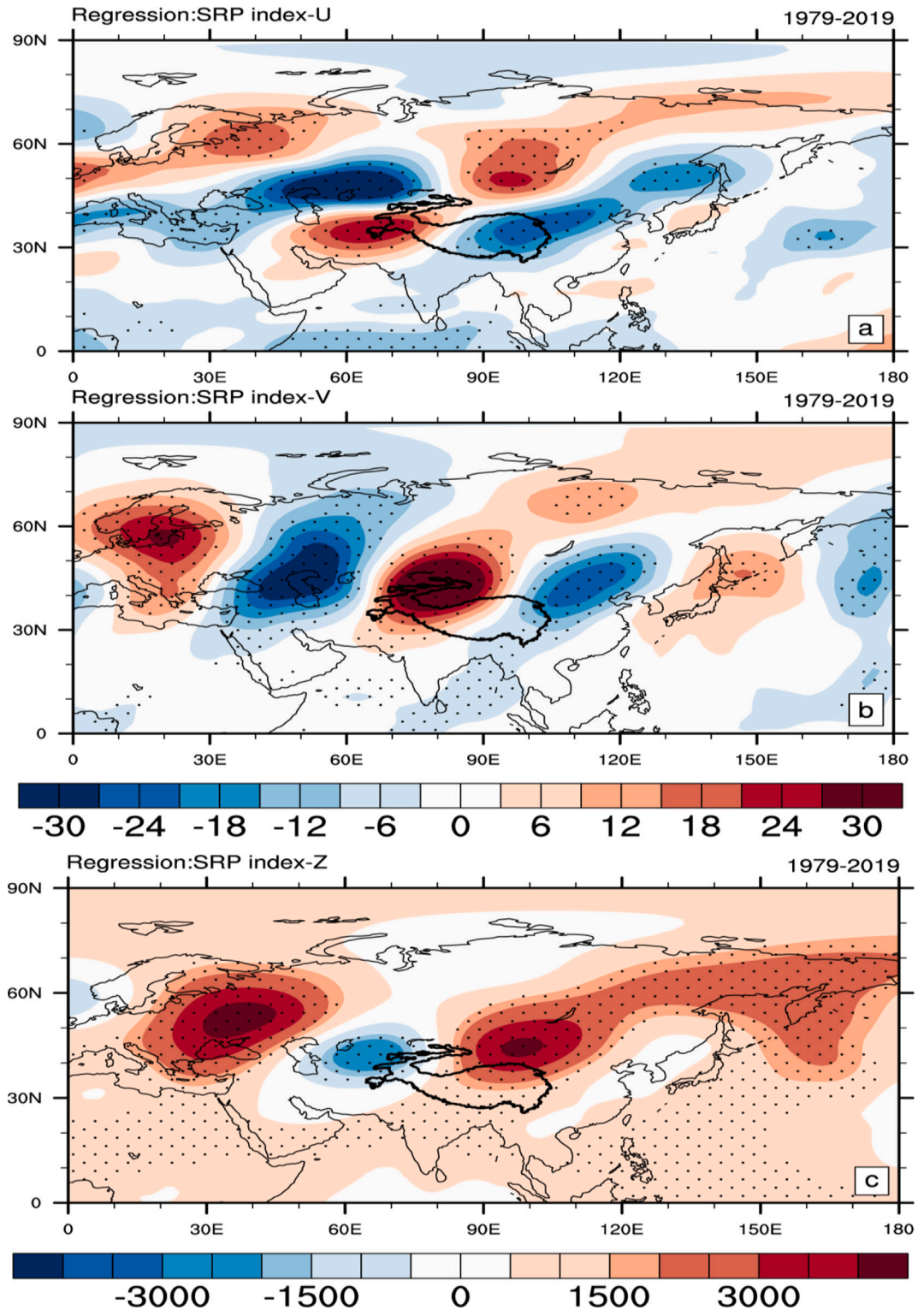

Fig. 4. Regression between SRP index, U—V wind speed, and geopotential height at 200 hPa. U and V are the zonal and meridional wind at 200 hPa, and Z is the geopotential height at 200 hPa. The dotted areas indicate statistically significant results at the 95% confidence level based on the Student's *t*-test. The black line indicates the TP region.

(a) Regression between the SRP index and zonal wind at 200 hPa.

(b) Regression between the SRP index and meridional wind at 200 hPa.

(c) Regression between the SRP index and geopotential height at 200 hPa.

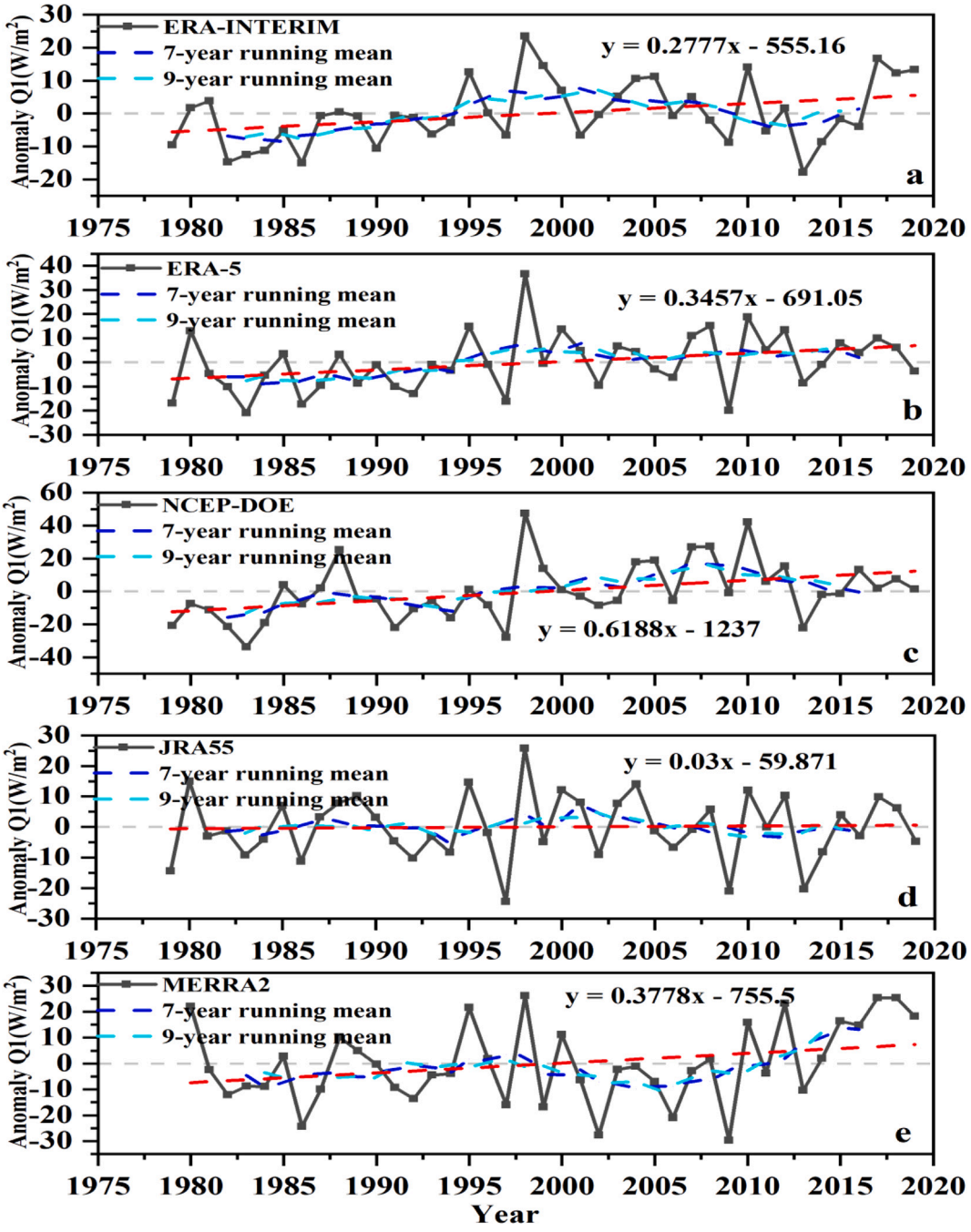

Fig. 5. Long-term variation of summer <Q1> anomaly calculated by (a) ERA-Interim (b) ERA-5 (c) NCEP-DOE (d) JRA-55 (e) MERRA2 from 1979 to 2019. Unit: $W \cdot m^{-2}$. The red line represents the trend line, the blue line represents the 7-year running mean <Q1>, the cyan line represents the 9-year running mean <Q1>.

2010), we performed an empirical orthogonal function (EOF) analysis for meridional wind (V-wind) at 200 hPa over the Eurasian region during June–July-August (JJA) (Fig. 3). The leading EOF (EOF1) in the ERA-5 data shows a wave-like pattern from Western Europe to Eastern Asia (Fig. 3a) and accounts for 25.5% of the total variance. It is worth noting that there is a positive phase of the wave train over the western TP and a negative phase over the eastern TP that might affect the atmospheric circulation over the TP region. The principal component of this leading mode (SRP index) (Fig. 3b) shows a regime shift for the SRP around 1997, indicating a structural change of the SRP in this year. To confirm whether this shift point is an obvious turning point, we used the Mann-Kendell test (MK-test) of the SRP index, shown in Fig. 3c, to analyze the abrupt change point. It can be found that the statistics index UF and the UB line intersect around 1997, indicating a regime shift of this mode around 1997. This conclusion is consistent with the conclusion drawn using NCEP/NCAR and JRA-55 data (Wang et al., 2017; Hong et al., 2018), indicating that ERA-5 data can accurately describe the long-term change characteristics of the SRP in boreal summer. Since the nature of the SRP is a stationary Rossby wave trapped in the jet stream (Lu et al., 2002; Enomoto et al., 2003), the SRP index is used to regress the wind field and geopotential height field at 200 hPa. These regressions indicated an obvious SRP over the Eurasia, which is significant at the 95% confidence level (Fig. 4a-c). This conclusion illustrates that ERA-5 data can capture the spatial structure of the summer SRP over Eurasia.

In summary, an obvious stationary RWT exists over Eurasia and this

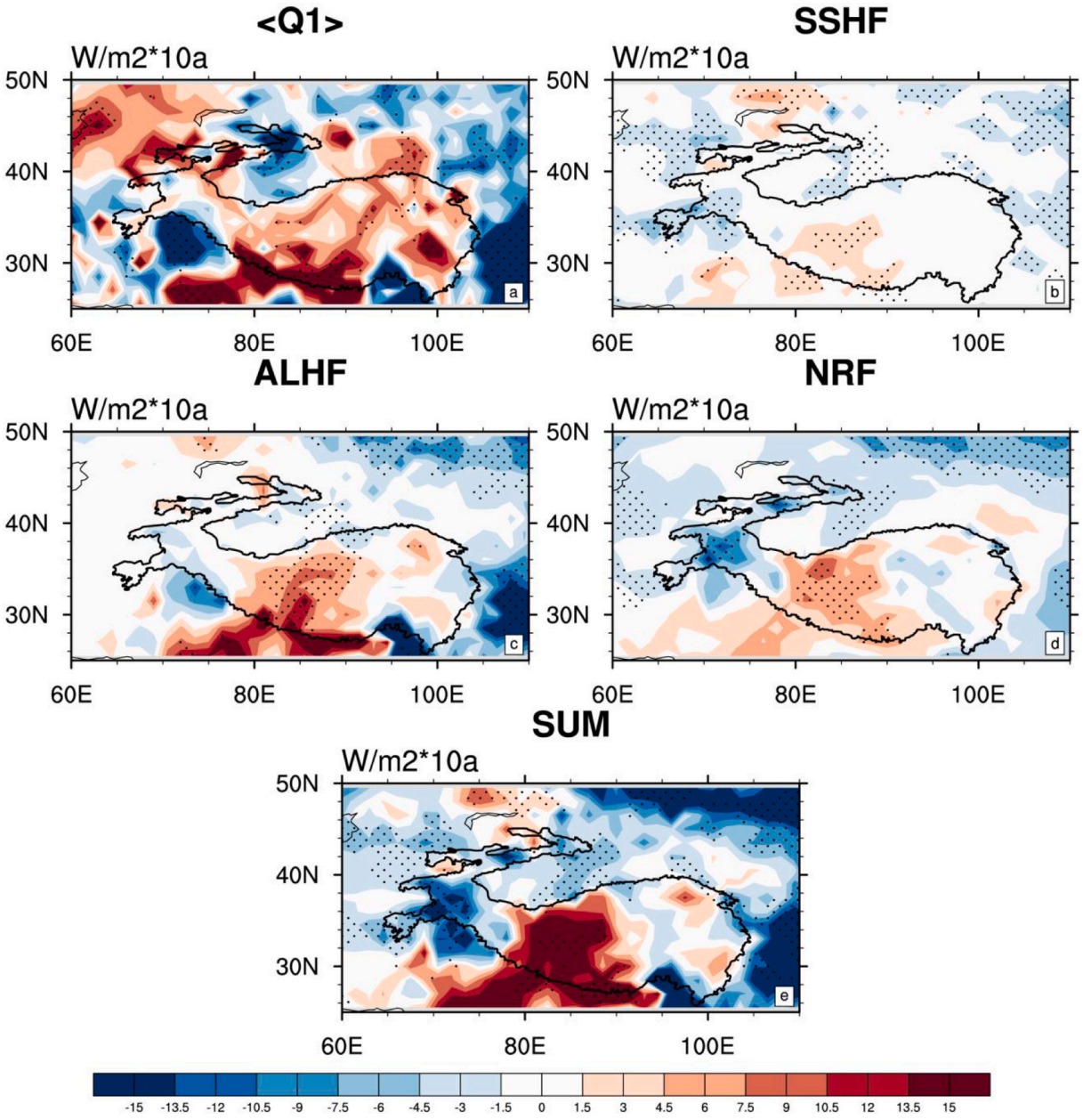

Fig. 6. The spatial distributions of the decadal change rate of (a) <Q1> (b) SSHF (c) ALHF (d) NRF and (e) their sum for increasing rate in JJA from 1979 to 2019 by ERA-5 data. Unit: $W \cdot m^{-2} \cdot (10a)$. The dotted areas indicate statistically significant results at the 95% confidence level based on the Student's *t*-test. The black line indicates the TP region.

is the pattern known as the SRP. Part of that pattern is located above the TP region, showing opposite phases over the eastern and western TP. Besides, the SRP exists an obvious interdecadal characteristic in the summer Eurasia. The SRP index shows an obvious increasing trend, with a regime shift around 1997, which might be influenced by SSAT in the North Atlantic, Atlantic Multidecadal Oscillation and the northeastern ISM anomaly (Wang et al., 2017; Piao et al., 2017; Zhou et al., 2019; Liu et al., 2020).

4.2. *Interdecadal variation characteristics of summer <Q1> over the TP region*

Previous studies mainly focused on the relationship between summer <Q1> on the TP and the ASM systems (Wu et al., 2015). The relationship between the SRP and the summer <Q1> in the TP region is rarely studied, even though the SRP is a large-scale teleconnection pattern in the northern hemisphere during summer. To further investigate the relationship between the SRP and the summer <Q1> on the TP, we calculate the summer <Q1> with ERA-5 reanalysis data to analyze the long-term variation characteristics of <Q1> over the TP region. Besides, other 4 reanalysis datasets are also used to verify the long-term change trend of the summer <Q1> in the TP.

Fig. 5 shows the long-term characteristics of the summer <Q1> anomaly from 1979 to 2019. The interannual variation of summer <Q1> of all reanalysis data shows obvious increasing trends during this period except JRA-55. We also analyzed the 7-year and 9-year running means of the <Q1> anomaly to filter out the interannual component and focus on the characteristics of interdecadal variability. The interdecadal <Q1> of ERA-5, ERA-Interim and NCEP-DOE are similar to the SRP index, while others didn't show such characteristics.

Luo and Yanai (1984) illustrated that there are two methods to calculate <Q1>. The first method is to calculate <Q1> from the

Table 4
The Correlation coefficients between <Q1> and SRP index on the different time scale in ERA-5 data.

correlation coefficients	Annual (SRP index)	7-year running mean (SRP index)	9 year running mean (SRP index)
Annual (Q1)	0.241	0.43**	0.411**
7-year running mean (Q1)	0.289	0.814**	0.875**
9-year running mean (Q1)	0.356*	0.804**	0.871**

*: 95%significance test. **:99% significance test.

perspective of energy balance through the thermodynamic equation. The other is to sum the surface sensible heat flux (SSHF), atmospheric latent heat flux (ALHF), and net radiation flux (NRF) in the air column to calculate <Q1>. To analyze the long-term variations of <Q1> more comprehensively, we have made a comparative analysis of <Q1> calculated by the two methods with ERA-5 data (Fig. 6). We found that the distribution characteristics of the change rate of the summer <Q1> calculated by the two methods are relatively consistent in the TP region (Fig. 6a and e). That is, both show a clear upward trend in the main plateau area. Since the <Q1> is mainly determined by SSHF, ALHF and NRF, the distribution characteristics of the interdecadal change rate of those components are also investigated in the TP region (Fig. 6b-d). We applied a linear fit to the time series of each component, with the slope indicating the rate of interdecadal change.

The Summer <Q1> over the whole TP region shows an increasing trend, especially over the central TP and southern slope of the Himalayas (Fig. 6a, e), which is similar to the trend of ALHF over the TP region (Fig. 6c). This illustrates that summer <Q1> is mainly affected by the latent heat release from the condensation of summer precipitation. Meanwhile, the NRF would also increase the <Q1>, but the impact of the NRF is weaker than that of the ALHF (Fig. 6d). Compared with ALHF and NRF, SSHF has almost no influence on <Q1> in summer (Fig. 6b). The sum of these three parts (SSHF, ALHF and NRF) (Fig. 6e) shows similar distribution characteristics to <Q1> (Fig. 6a), indicating that the distribution characteristics of the <Q1> are reliable over the TP.

4.3. Relationship between the interdecadal variation of the SRP and summer <Q1> over the TP region

Since the SRP index and the summer <Q1> have relatively similar variation characteristics, to further investigate their relationship, the correlation coefficients between them are investigated and shown in Table 4. On the interannual scale, there have no correlations between the SRP index and summer <Q1>, the coefficient was only 0.241. However, the coefficients of 7-year and 9-year running mean reach 0.814 and 0.871, and both are significant at the 99% confidence level, which means the SRP is highly correlated with the summer <Q1> on the interdecadal scale.

Our former results indicated that summer <Q1> was highly related to the atmospheric latent heat released by the precipitation condensation. Thus, regression analysis between SRP index, precipitation, and <Q1> are performed to investigate their relationship in the TP region (Fig. 7). Over the whole TP region, the SRP, precipitation, and summer <Q1> are highly correlated, especially in the central TP (Fig. 7). The similar distribution patterns illustrated in these two figures indicate that the latent heat released by the precipitation condensation is the main component of the summer <Q1> in the TP region. Meanwhile, two highly correlated regions of those components appear in the western and central TP and these locations are consistent with the distribution area of the SRP. This indicates that the SRP might affect local <Q1> through precipitation over the TP region.

4.4. Impact of the SRP on the interdecadal change in summer <Q1> over the TP region

Although there are many studies on the factors influencing the variation in summer <Q1> (e.g. Zhao and Chen, 2001; Wu et al., 2007), few studies have focused on the relationship between the boreal summer SRP and <Q1> over the TP region. In this study, we found that the SRP would also influence the summer <Q1> in the TP region. However, possible mechanisms still require further investigation.

Our interdecadal analysis of the SRP index reveals a remarkable difference between 1979-1996 and 1997–2019. This difference is similar to the conclusion of Wang et al. (2017) and Liu et al. (2020). Liu et al. (2020) illustrated that this regime shift of the SRP is attributed to an enhanced impact of precipitation anomalies over the northeastern Indian summer monsoon (ISM) around the late 1990s. Also, the SSTA in the northwestern Atlantic is one of the influencing factors that cause changes to the SRP (Zhou et al., 2019).

The interdecadal variation of the SRP reveals that the SRP fluctuates from the negative phase to the positive phase, with strong negative anomalies appearing before 1996 and strong positive anomalies after this date. Based on the interdecadal variation of the SRP, we select 1979–1996 as the negative phase of the SRP (NPS), and the period 1997–2019 as the positive phase of the SRP (PPS), with which to conduct a comparative analysis.

To better understand the impact of the variation of the SRP on summer <Q1>, we calculated the differences in the wind field and <Q1> in the NPS and the PPS (PPS minus NPS) at 500 hPa (Fig. 8). A series of wind field cyclonic (anticyclonic) anomalies are observed along Eurasia at 200 hPa, which are consistent with the spatial structure of the SRP (Figure is not shown). This implies that the shift of the SRP will trigger an abnormal cyclone (anticyclone) in the wind field along Eurasia. The shift of the SRP generated an anomalous anticyclonic wind field near Lake Baikal at 500 hPa (Fig. 8a), resulting in an anomalous wind field from east to west on the TP, meanwhile, the water vapor showed similar pattern at 500 hPa. This indicated that the moisture would transport through the eastern boundary of the TP during the NPS and this phenomenon was inhibited during the PPS, which would increase the content of water vapor over the TP region (Zhou et al., 2019). Besides, the southerly wind and water vapor increased across the southern boundary of the TP, which brought abundant moisture into the TP, increased the atmospheric moisture content in the TP.

Accompanying the interdecadal shift of the SRP, the vertical velocity differences (dp/dt) also experience a corresponding change (Fig. 9). The dp/dt differences are positive at 70–80°E and 92–96°E, which correspond to the downward vertical motion in the troposphere. The dp/dt is negative at 65–70°E, 83–92°E, and 96–105°E. In this way, the corresponding vertical motion is upward. In the condition of abundant water vapor, the change of vertical motion will create a large-scale favorable environment for an increase in precipitation, and eventually release a large amount of ALHF and affect the increase of <Q1> in the TP region.

In summary, the possible mechanism of how the SRP affects the summer <Q1> over the TP can be summarized as follows: in summer, there exist an SRP over Eurasia, which transferred from a negative phase to a positive phase around 1997 on the interdecadal scale. This regime shift might be caused by Atlantic Multidecadal Oscillation, SSTA in the northwestern Atlantic and precipitation anomalies over the northeastern Indian summer monsoon (ISM) (Wang et al., 2017; Zhou et al., 2019; Liu et al., 2020). The regime shift of the SRP would have produced a significant anomalous anticyclonic wind field over Lake Baikal at 500 hPa, which would have inhibited water vapor transport through the eastern boundary of the TP. Meanwhile, Indian Summer Monsoon (ISM) would also transport the moisture through the southern boundary of the TP and increased the contents of water vapor over the TP. As the moisture content increased, the change of vertical motion over the TP would have produced plenty of precipitation, eventually affecting the change of summer <Q1> in the TP region (Fig. 10).

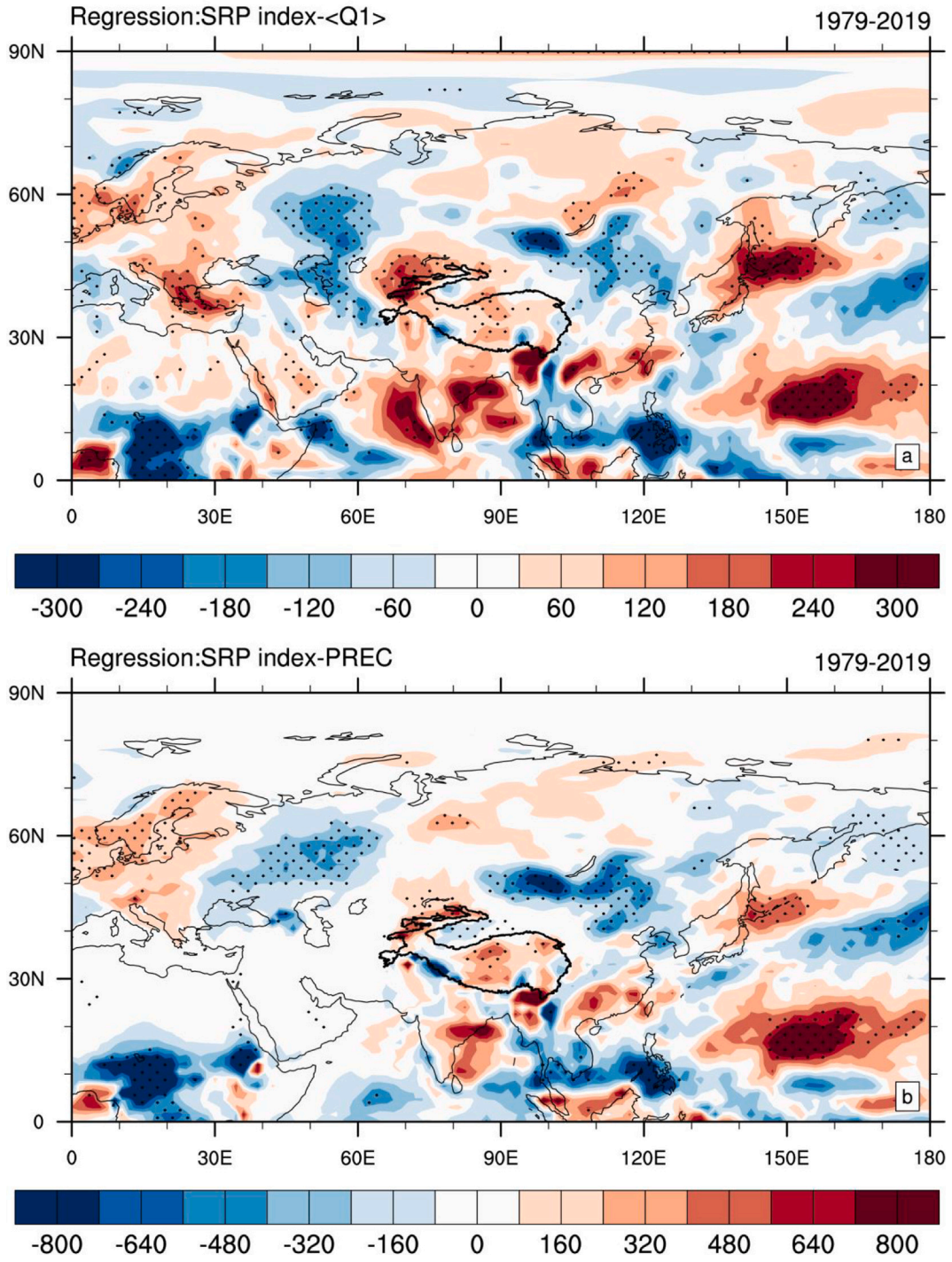

Fig. 7. Regression relationships between SRP index and (a) summer <Q1>, (b) summer precipitation from 1979 to 2019. The dotted area indicates statistically significant at the 95% confidence level based on the Student's *t*-test. The black line indicates the TP region.

5. Discussion

Since the <Q1> have great influences on the climate pattern of China, East Asia and northern hemisphere, it's long-term characteristics attracted much attention (Jiang et al., 2016; Xie and Wang, 2019; Han et al., 2019). Besides, the possible mechanisms for variations in <Q1> over the TP are also investigated (Zhao et al., 2018; Ren et al., 2019; Xiao et al., 2019; Lu et al., 2019). Using 5 reanalysis datasets, this study analyzed the possible relationship between the summer SRP and <Q1> in the TP region over the past four decades.

Using our radiosonde data collected in May and July 2019, 5 reanalysis data (ERA-Interim, ERA-5, NCEP-DOE, MERRA2 and JRA-55) was verified over the 4 sites in the TP region. Former studies have verified several reanalysis data in the TP (Bao and Zhang, 2013; Gao et al., 2014; Hu and Yuan, 2021), however, few of them verified those reanalysis datasets together to compare their accuracy in different parts of the TP. Our verification illustrated that there exist some differences between those 5 datasets over the TP region due to the differences in the horizontal and vertical resolution among them. Our result indicated that ERA-5 have the smallest bias and highest correlation coefficients in the 4 sites, Thus, it was used to analyze the long-term characteristic of the summer SRP and the <Q1>, as well as their correlations, even though it

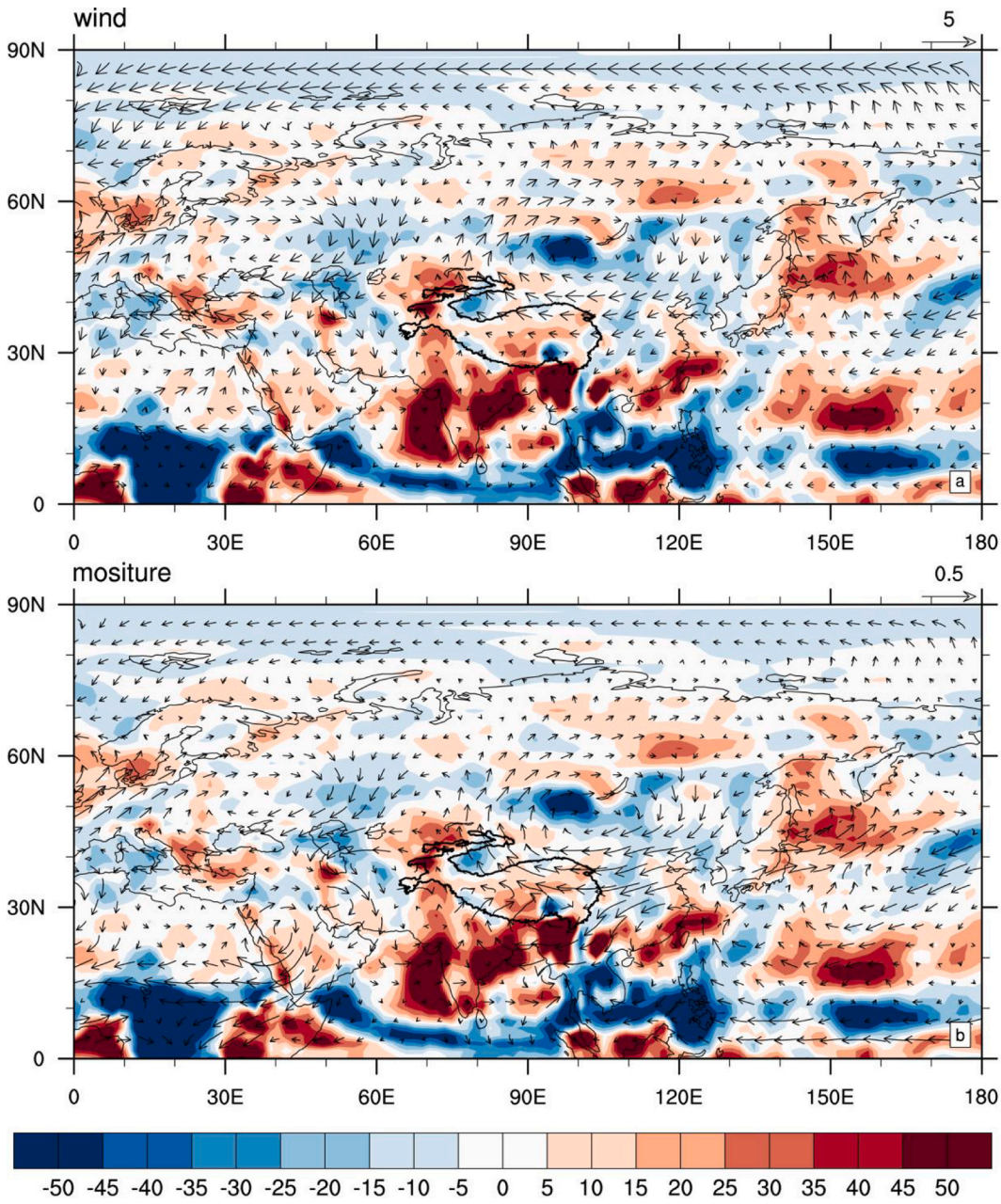

Fig. 8. The differences over 1979–1996 (NPS) and 1997–2019 (PPS) (PPS minus NPS) for the distribution of the <Q1> (shading, unit: Wm^{-2}) and (a) wind field (arrows, unit: ms^{-1}) (b) water vapor flux (arrows, unit: g $(s*hPa*cm)^{-1}$) at 500 hPa. The black line indicates the TP region.

has shorter time series than other datasets.

As a wave train system on the planetary scale over the northern hemisphere in summer, the SRP has an important influence on the regional climate of the northern hemisphere (Huang et al., 2011; Su and Lu, 2014; Hong and Lu, 2016; Hong et al., 2017). Since it's importance in the climate system, the long-term characteristics of the SRP are also investigated (Wang et al., 2017; Hong et al., 2018). Their studies illustrated that the SRP index experiences two regime shifts on the interdecadal time scale, in 1972 and 1997. our study shows that the SRP fluctuates from the negative phase to the positive phase and the shift point is around 1997, which is consistent with their conclusion. However, due to the shorter time scale of ERA-5 data, we only captured the regime shift in 1997, thus, we mainly focus on this regime shift of the SRP and it's influence on the summer <Q1> of the TP.

The reasons for the regime shift of the SRP in the middle 1990s have caused a lot of controversies. For example, Wang et al. (2017) illustrated that the Atlantic Multidecadal Oscillation is a plausible driver of the SRP. Piao et al., (2017) analyzed the SRP shift in the late 1990s, showing that the summer SSTA in the North Atlantic would induce the observed SRP variation over Eurasia. Zhou et al. (2019) also found this anomalous wave energy propagates from the extratropical North Atlantic towards East Asia. They found that this anomalous wave train is related to the variation of SST in the northwestern Atlantic. However, Liu et al. (2020) found that the reshaping of the SRP around the late 1990s is attributed to an enhanced impact of precipitation anomalies over the northeastern Indian summer monsoon (ISM). Their result implies that the summer SSTA in the North Atlantic and the northeastern ISM anomaly are the main reasons for the regime shift of the SRP in 1997. Those results indicated that the interdecadal variation of the SRP might be influenced by the interaction of multiple systems. However, our study mainly focuses on the relationship between the SRP and summer <Q1> in the TP, the possible influence factor for the SRP variation will be discussed in

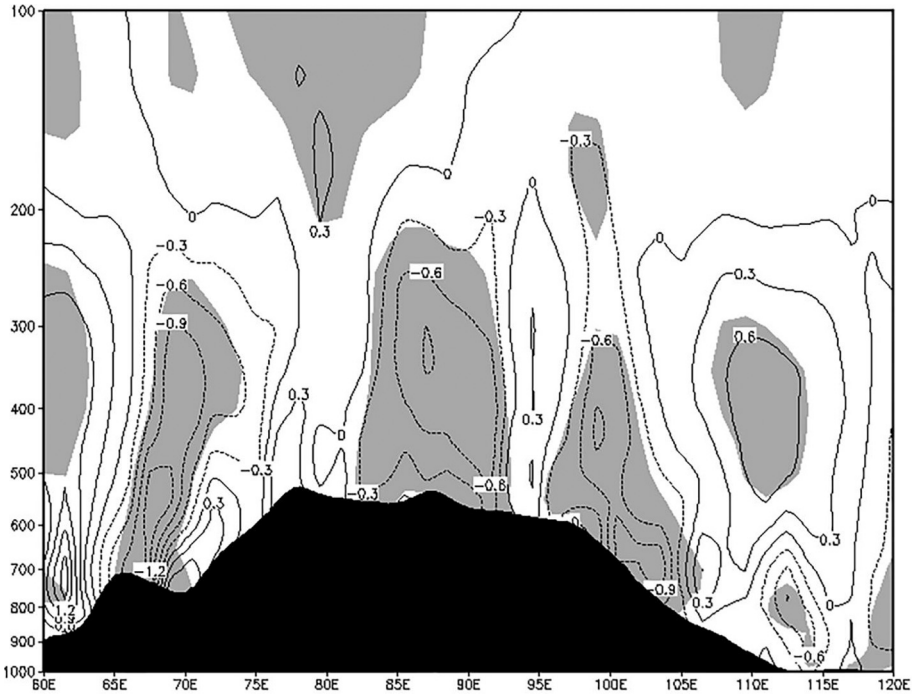

Fig. 9. The longitude-height cross section of the difference between 19791996 (NPS) and 1997-2019 (PPS) for the vertical velocity (dp/dt) (10^{-2} hPa s^{-1}) averaged for 30–40°N in summer. The shading indicates statistically significant results at the 95% confidence level based on the Student's *t*-test. The black area indicates the TP region.

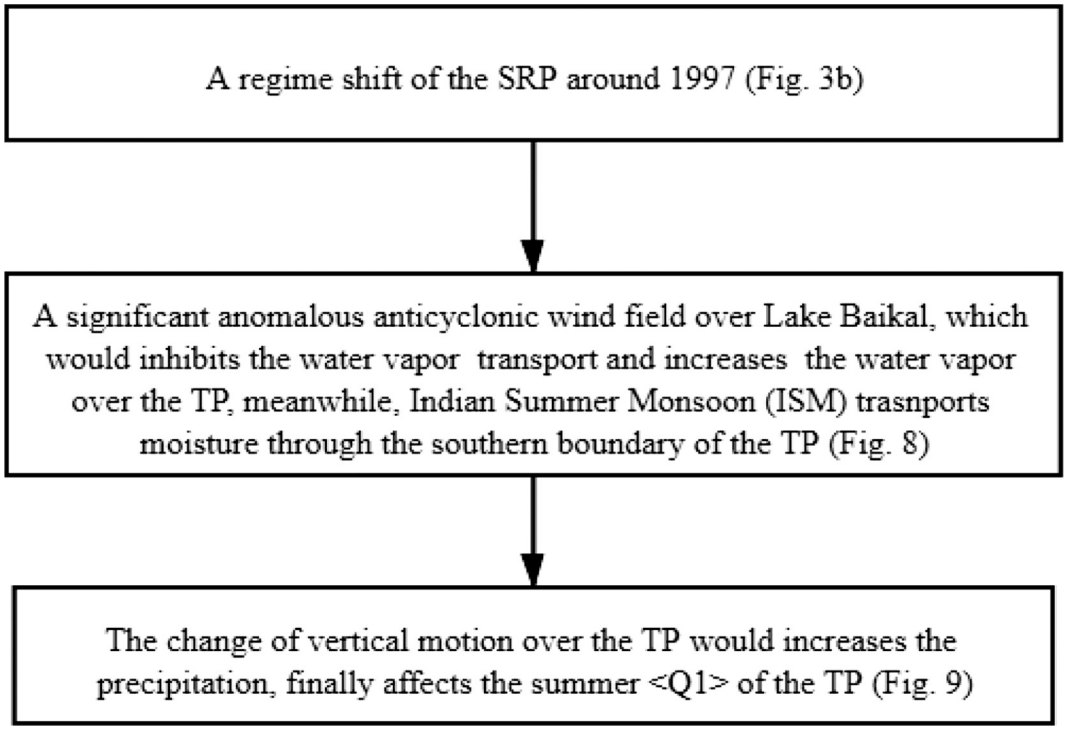

Fig. 10. Schematic diagram showing the possible mechanisms for the interdecadal variations of the summer SRP affecting <Q1> over the TP.

the future study.

As a collection of energy in the atmospheric air column, the variation of the <Q1> in the TP would have a great impact on the atmospheric circulation system in the TP, China and East Asia (Li and Yanai, 1996; Hsu and Liu, 2003; Qin et al., 2009; Chen et al., 2015). Previous studies have shown that summer <Q1> have shown an increasing trend during the past few decades in the TP region (Yang et al., 2011; Xie and Wang, 2019). However, their method of calculating the <Q1> is to calculate sensible heat (SH), latent heat (LH) and net radiation (RAD) separately and sum them to get the energy in the entire atmospheric column. Different from their method, we used to equations of Luo and Yanai (1984), the advantages of this method is that it can not only calculate the

Table 5
The Correlation coefficients between <Q1> and SRP on different time scale among different datasets.

Correlation coefficients	Annual ERA-5 <Q1>	Annual Interim <Q1>	Annual NCEP-DOE <Q1>	Annual JRA-55 <Q1>	Annual MERRA2 <Q1>
Annual(ERA-5 SRP index)	0.241	0.358*	0.460**	0.109	0.087
correlation coefficients	7-year running ERA-5 <Q1>	7-year running Interim <Q1>	7-year running NCEP-DOE <Q1>	7-year running JRA-55 <Q1>	7-year running MERRA2 <Q1>
7-year running (ERA-5 SRP index)	0.814**	0.596**	0.808**	0.235	0.340*
correlation coefficients	9-year running ERA-5 <Q1>	9-year running Interim <Q1>	9-year running NCEP-DOE <Q1>	9-year running JRA-55 <Q1>	9-year running MERRA2 <Q1>
9-year running (ERA-5 SRP index)	0.0.871**	0.628**	0.889**	0.167	0.255

*: 95%significance test. **:99% significance test.

<Q1> in the entire atmospheric column but also calculate it on different levels. In our study, we mainly focused on the summer <Q1> of the entire atmospheric column, Thus the vertical structure of the summer <Q1> was not discussed in this study. Our study indicated that summer <Q1> calculated by 5 reanalysis datasets all showed upward trends from 1979 to 2019, which was similar to the conclusion of Xie and Wang (2019). This also confirms that the two methods are consistent with the heat source calculations in the TP area (Fig. 7). In this study, we mainly studied the interdecadal characteristics of the summer <Q1> in the entire atmospheric column, the <Q1> in different levels would be discussed in our future work.

Most of the previous studies studied the SRP and summer <Q1> separately, and few of them analyzed the correlations between them. Our study focuses on the correlation between them and found that the SRP is highly correlated with the summer <Q1> on the interdecadal scale. The correlation coefficients exceeded 0.8 and passed the 99% significance test (Table 4), which illustrated that the increasing of summer <Q1> was highly correlated to the regime shift of the SRP in 1997. Besides, the interdecadal variation of NCEP-DOE <Q1> and ERA-Interim <Q1> also show highly correlated with the SRP index of ERA-5 data, which illustrate that this correlation can be captured by multi-datasets (Table 5).

However, our work does have some limitations: even though we used radiosonde data in 4 sites in the TP to verifying the accuracy of 5 reanalysis datasets, the radiosonde data is still insufficient. Besides, our radiosonde data are all collected in 2019, and we lack data from different years for comparison and verification. Despite this, we still thought the verification is important in this study. Further, changes in summer <Q1> in the TP would be affected by many factors such as the soil moisture (Zhu et al., 2007), snow cover (Qian et al., 2003), South Asian high (Ren et al., 2019) etc. This study only focuses on the impact of the SRP on the summer <Q1> in the TP. Overall, this study provides an overall description of the relationship between SRP and summer <Q1> and it is of great significance to understand the variations characteristic of <Q1> in the TP region.

6. Conclusions

In this study, we investigated the interdecadal variation of the summer SRP and its relationship with the summer <Q1> over the TP region using 5 reanalysis data for a recent 41-year period. The results suggest that the SRP transitioned from a negative phase to a positive phase around 1997. This regime shift in the SRP might be caused by the Atlantic Multidecadal Oscillation, the SSTA in the northwestern Atlantic and abnormal precipitation over the northeastern ISM (Zhou et al., 2019; Liu et al., 2020). Meanwhile, the interdecadal variation of the SRP has a clear positive correlation with summer <Q1> in the TP region.

On the interdecadal scale, the summer <Q1> calculated by a variety of reanalysis data shows an upward.trend. This variation is closely associated with the change of precipitation. The interdecadal change of summer <Q1> is highly correlated with that of the SRP index. Further analysis shows that the shift in the summer SRP would have generated circulation anomalies in the Lake Baikal region at 500 hPa. These circulation anomalies will have limited water vapor transport through the eastern boundary of the TP during NPS, and have increased the water vapor transported by the Indian Summer Monsoon (ISM) through the southern boundary of the TP during PPS; this is one reason for the TP's transition from a dry stage to a wet stage (Zhou et al., 2019). Meanwhile, vertical air movement over the TP will lead to abundant precipitation due to the increased moisture, releasing a large amount of latent heat through the condensation of precipitation, eventually leading to the enhancement of <Q1> over the TP.

It is worth noting that the interdecadal variation of summer <Q1> over the TP is not only affected by the SRP, but also by many other factors, such as the ASM and ocean forcings (for example, ENSO and tropical SST). In the present paper, we only focused on the interdecadal change of summer <Q1> due to the RWT during summer over the TP in the past few decades. Future work should consider other forcings of the SRP and summer <Q1>.

Declaration of Competing Interest

The authors declare that they have no known competing financial interests or personal relationships that could have appeared to influence the work reported in this paper.

Acknowledgements

This study was supported by The National Key Basic Research Program (2018YFC1505701), the Second Tibetan Plateau Scientific Expedition and Research (STEP) program (2019QZKK0103), the Strategic Priority Research Program of Chinese Academy of Sciences, (No. XDA2006010103 and XDA19070301) and the National Natural Science Foundation of China (NSFC) (No. 41830650, 91837208, 41661144043). The authors express thanks to ECMWF for sharing reanalysis data sets, as well as to staff from the CAS comprehensive observation stations QOMS, NADORS, NADORS and SETORS for their very hard work collecting radiosonde observations over the TP and offering us these data. The reanalysis data in this paper can be download from the ECMWF website. A copy of the radiosonde data can be obtained through the corresponding authors. The authors declare no conflict of interest.

References

Bao, X.H., Zhang, F.Q., 2013. Evaluation of NCEP–CFSR, NCEP–NCAR, ERA-Interim, and ERA-40 reanalysis datasets against independent sounding observations over the Tibetan Plateau. J. Clim. 26, 206–214.
Chen, G.S., Huang, R.H., 2012. Excitation mechanisms of the teleconnection patterns affecting the July precipitation in Northwest China. J. Clim. 25, 7834–7851.
Chen, J.H., Wu, X.Q., Yin, Y., Xiao, H., 2015. Characteristics of heat sources and clouds over eastern China and the Tibetan Plateau in boreal summer. J. Clim. 28, 7279–7296.
Chen, W., Feng, J., Wu, R., 2013. Roles of ENSO and PDO in the link of the East Asian winter monsoon to the following summer monsoon. J. Clim. 26 (2), 622–635.
Chowdary, J.S., Hu, K., Srinivas, G., Kosaka, Y., Wang, L., Rao, K.K., 2019. The Eurasian jet streams as conduits for East Asian monsoon variability. Curr. Clim. Change. Rep. 5 (3), 233–244.

Cui, Y.F., Duan, A.M., Liu, Y.M., Wu, G.X., 2015. Interannual variability of the spring atmospheric heat source over the Tibetan Plateau forced by the North Atlantic SSTA. Clim. Dyn. 45, 1617–1634.
Dee, D.P., Uppala, S.M., Simmons, A.J., Berrisford, P., Poli, P., Kobayashi, S., Andrae, U., Balmaseda, M.A., Balsamo, G., Bauer, D.P., 2011. The ERA-Interim reanalysis: configuration and performance of the data assimilation system. Quart. J. Roy. Meteor. Soc. 137, 553–597.
Ding, Q.H., Wang, B., 2005. Circumglobal teleconnection in the Northern Hemisphere summer. J. Clim. 18, 3483–3505.
Ding, Q.H., Wang, B., Wallace, J.M., Branstator, G., 2011. Tropical–extratropical teleconnections in boreal summer: observed interannual variability. J. Clim. 24, 1878–1896.
Duan, A.M., Wu, G.X., 2005. Role of the Tibetan Plateau thermal forcing in the summer climate patterns over subtropical Asia. Clim. Dyn. 24, 793–807.
Duan, A.M., Wang, M.R., Xiao, Z.X., 2014. Uncertainties in quantitatively estimating the atmospheric heat source over the Tibetan Plateau. Atmos. Oceanic. Sci. Lett. 7, 28–33.
Enomoto, T., 2004. Interannual variability of the Bonin high associated with the propagation of Rossby waves along the Asian jet. J. Meteor. Soc. Japan. Ser. II 82, 1019–1034.
Enomoto, T., Hoskins, B.J., Matsuda, Y., 2003. The formation mechanism of the Bonin high in August. Quart. J. Roy. Meteor. Soc. 129, 157–178.
Feng, J., Wang, L., Chen, W., 2014. How does the East Asian summer monsoon behave in the decaying phase of El Niño during different PDO phases? J. Clim. 27 (7), 2682–2698.
Gao, L., Hao, L., Chen, X.W., 2014. Evaluation of ERA-interim monthly temperature data over the Tibetan Plateau. J. Mt. Sci. 11, 1154–1168.
Gelaro, R., McCarty, W., Suárez, M.J., Todling, R., Molod, A., Takacs, L., Randles, C.A., Darmenov, A., Bosilovich, M.G., Reichle, R., Wargan, K., Coy, L., Cullather, R., Draper, C., Akella, S., Buchard, V., Conaty, A., Silva, A.M., Gu, W., Kim, G.K., Koster, R., Lucchesi, R., Merkova, D., Nielsen, J.E., Partyka, G., Pawson, S., Putman, W., Rienecker, M., Schubert, S.D., Sienkiewicz, M., Zhao, B., 2017. The modern-era retrospective analysis for research and applications, version 2 (MERRA-2). J. Clim. 30 (14), 5419–5454.
Han, Y.Z., Ma, W.Q., Ma, Y.M., Sun, C.Y., 2019. Variations of surface heat fluxes over the Tibetan Plateau before and after the onset of the south Asian summer monsoon during 1979–2016. J. Meteorol. Res. 33, 491–500.
Hersbach, H., Bell, B., Berrisford, P., Horányi, A., Muñoz, J., Nicolas, J., Radu, R., Schepers, D., Simmons, A., Soci, C., Dee, D., 2019. Global reanalysis: goodbye ERA-interim, hello ERA-5. ECMWF Newslett. 159, 17–24.
Hong, X.W., Lu, R.Y., 2016. The meridional displacement of the summer Asian jet, Silk Road pattern, and tropical SST anomalies. J. Clim. 29, 3753–3766.
Hong, X.W., Lu, R.Y., Li, S.L., 2017. Amplified summer warming in Europe–West Asia and Northeast Asia after the mid-1990s. Environ. Res. Lett. 12, 094007.
Hong, X.W., Xue, S.H., Lu, R.Y., Liu, Y.Y., 2018. Comparison between the interannual and decadal components of the Silk Road pattern. Atmos. Oceanic. Sci. Lett. 11, 270–274.
Hsu, H.H., Liu, X., 2003. Relationship between the Tibetan Plateau heating and East Asian summer monsoon rainfall. Geophys. Res. Lett. 30.
Hu, X., Yuan, W., 2021. Evaluation of ERA-5 precipitation over the eastern periphery of the Tibetan Plateau from the perspective of regional rainfall events. Int. J. Climatol. 1-13.
Huang, G., Liu, Y., Huang, R.H., 2011. The interannual variability of summer rainfall in the arid and semiarid regions of northern China and its association with the Northern Hemisphere circumglobal teleconnection. Adv. Atmos. Sci. 28, 257–268.
Jiang, X.W., Li, Y.Q., Yang, S., Yang, K., Chen, J.W., 2016. Interannual variation of summer atmospheric heat source over the Tibetan Plateau and the role of convection around the western Maritime Continent. J. Clim. 29, 121–138.
Kanamitsu, M., Ebisuzaki, W., Woollen, J., Yang, S.K., Hnilo, J.J., Fiorino, M., Potter, G. L., 2002. NCEP-DOE AMIP-II Reanalysis (R-2). Bull. Amer. Meteor. Soc. 83, 1631–1643.
Kobayashi, S., Ota, Y., Harada, Y., Ebita, A., Moriya, M., Onoda, H., Onogi, K., Kamahori, H., Kobayashi, C., Endo, H., Miyaoka, K., Takahashi, K., 2015. The JRA-55 reanalysis: general specifications and basic characteristics. J. Meteor. Soc. Japan 93, 5–48.
Kosaka, Y., Nakamura, H., Watanabe, M., Kimoto, M., 2009. Analysis on the dynamics of a wave-like teleconnection pattern along the summertime Asian jet based on a reanalysis dataset and climate model simulations. J. Meteor. Soc. Japan. Ser. II 87, 561–580.
Kosaka, Y., Chowdary, J.S., Xie, S.P., Min, Y.M., Lee, J.Y., 2012. Limitations of seasonal predictability for summer climate over East Asia and the Northwestern Pacific. J. Clim. 25, 7574–7589.
Kumar, K.K., Rajagopalan, B., Cane, M.A., 1999. On the weakening relationship between the Indian monsoon and ENSO. Science 284 (5423), 2156–2159.
Li, C.F., Yanai, M., 1996. The onset and interannual variability of the Asian summer monsoon in relation to land–sea thermal contrast. J. Clim. 9, 358–375.
Liu, X.D., Chen, B.D., 2000. Climatic warming in the Tibetan Plateau during recent decades. Int. J. Climatol. 20, 1729–1742.
Liu, Y., Zhou, W., Qu, X., Wu, R.G., 2020. An Interdecadal Change of the Boreal Summer Silk Road Pattern around the late 1990s. J. Clim. 33, 7083–7100.
Lu, M.M., Huang, B.H., Li, Z.N., Yang, S., Wang, Z.Q., 2019. Role of Atlantic air–sea interaction in modulating the effect of Tibetan Plateau heating on the upstream climate over Afro-Eurasia–Atlantic regions. Clim. Dyn. 53, 509–519.
Lu, R.Y., Oh, J.H., Kim, B.J., 2002. A teleconnection pattern in upper-level meridional wind over the North African and Eurasian continent in summer. Tellus A: Dyn. Meteorol. Oceanogr. 54, 44–55.
Luo, H.B., Yanai, M., 1984. The large-scale circulation and heat sources over the Tibetan Plateau and surrounding areas during the early summer of 1979. Part II: Heat and moisture budgets. Mon. Weather Rev. 112, 966–989.
Niu, T., Chen, L.X., Zhou, Z.J., 2004. The characteristics of climate change over the Tibetan Plateau in the last 40 years and the detection of climatic jumps. Adv. Atmos. Sci. 21, 193–203.
Piao, J.L., Chen, W., Wei, K., Liu, Y., Graf, H.F., Ahn, J.B., Pogoreltsev, A., 2017. An abrupt rainfall decrease over the Asian inland plateau region around 1999 and the possible underlying mechanism. Adv. Atmos. Sci. 34, 456–468.
Qian, Y.F., Zheng, Y.Q., Zhang, Y., Miao, M., 2003. Responses of China's summer monsoon climate to snow anomaly over the Tibetan Plateau. Int. J. Climatol. 23, 593–613.
Qin, J., Yang, K., Liang, S.L., Guo, X.F., 2009. The altitudinal dependence of recent rapid warming over the Tibetan Plateau. Clim. Chang. 97, 321.
Qiu, J., 2008. China: the third pole. Nature. News. 454, 393–396.
Ren, R.C., Zhu, C.D., Cai, M., 2019. Linking quasi-biweekly variability of the South Asian high to atmospheric heating over Tibetan Plateau in summer. Clim. Dyn. 53, 3419–3429.
Sato, N., Takahashi, M., 2006. Dynamical processes related to the appearance of quasi-stationary waves on the subtropical jet in the midsummer Northern Hemisphere. J. Clim. 19, 1531–1544.
Shi, Q., Liang, S., 2014. Surface-sensible and latent heat fluxes over the Tibetan Plateau from ground measurements, reanalysis, and satellite data. Atmos. Chem. Phys. 14.
Song, F.F., Zhou, T.J., Wang, L., 2013. Two modes of the Silk Road pattern and their interannual variability simulated by LASG/IAP AGCM SAMIL2.0. Adv. Atmos. Sci. 30, 908–921.
Su, Q., Lu, R.Y., 2014. Teleconnection between rainfall over South China and the east European Plain in July and August. Theor. Appl. Climatol. 118, 185–194.
Tao, S.Y., Ding, Y.H., 1981. Observational evidence of the influence of the Qinghai-Xizang (Tibet) Plateau on the occurrence of heavy rain and severe convective storms in China. Bull. Amer. Meteor. Soc. 62, 23–30.
Wang, H., Wang, B., Huang, F., Ding, Q.G., Lee, J.Y., 2012. Interdecadal change of the boreal summer circumglobal teleconnection (1958–2010). Geophys. Res. Lett. 39.
Wang, L., Xu, P.Q., Chen, W., Liu, Y., 2017. Interdecadal variations of the Silk Road pattern. J. Clim. 30, 9915–9932.
Wu, B., Lin, J.S., Zhou, T.J., 2016. Interdecadal circumglobal teleconnection pattern during boreal summer. Atmos. Sci. Lett. 17, 446–452.
Wu, G.X., Liu, Y.M., Zhang, Q., Duan, A.M., Wang, T.M., Wan, R.J., Liu, X., Li, W.P., Wang, Z.Z., Liang, X.Y., 2007. The influence of mechanical and thermal forcing by the Tibetan Plateau on Asian climate. J. Hydrometeorol. 8, 770–789.
Wu, G.X., Duan, A.M., Liu, Y.M., Mao, J.Y., Ren, R.C., Bao, Q., He, B., Liu, B.Q., Hu, W.T., 2015. Tibetan Plateau climate dynamics: recent research progress and outlook. Natl. Sci. Rev. 2, 100–116.
Xiao, Z.X., Duan, A.M., Wang, Z.Q., 2019. Atmospheric heat sinks over the western Tibetan Plateau associated with snow depth in late spring. Int. J. Climatol. 39, 5170–5180.
Xie, Z.L., Wang, B., 2019. Summer atmospheric heat sources over the Western–central Tibetan Plateau: an integrated analysis of multiple reanalysis and satellite datasets. J. Clim. 32, 1181–1202.
Yanai, M., Li, C.F., 1994. Mechanism of heating and the boundary layer over the Tibetan Plateau. Mon. Weather Rev. 122, 305–323.
Yanai, M., Li, C.F., Song, Z.S., 1992. Seasonal heating of the Tibetan Plateau and its effects on the evolution of the Asian summer monsoon. J. Meteor. Soc. Japan. Ser. II 70, 319–351.
Yang, K., Guo, X., He, J., Qin, J., Koike, T., 2011. On the climatology and trend of the atmospheric heat source over the Tibetan Plateau: an experiments-supported revisit. J. Clim. 24 (5), 1525–1541.
Yasui, S., Watanabe, M., 2010. Forcing processes of the summertime circumglobal teleconnection pattern in a dry AGCM. J. Clim. 23, 2093–2114.
Zhao, P., Chen, L.X., 2001. Climatic features of atmospheric heat source/sink over the Qinghai-Xizang Plateau in 35 years and its relation to rainfall in China. Sci. China. Ser. D. 44, 858–864.
Zhao, Y., Duan, A.M., Wu, G.X., 2018. Interannual variability of late-spring circulation and diabatic heating over the Tibetan Plateau associated with Indian Ocean forcing. Adv. Atmos. Sci. 35, 927–941.
Zhou, C.Y., Zhao, P., Chen, J.M., 2019. The interdecadal change of summer water vapor over the Tibetan Plateau and associated mechanisms. J. Clim. 32, 4103–4119.
Zhu, W.Q., Chen, L.X., Zhou, Z.J., 2001. Several characteristics of contemporary climate change in the Tibetan Plateau. Sci. China. Ser. D. 44, 410.
Zhu, X.Y., Liu, Y.M., Wu, G.X., 2012. An assessment of summer sensible heat flux on the Tibetan Plateau from eight data sets. Sci. China. Ser. D. 55, 779–786.
Zhu, Y.X., Ding, Y.H., Xu, H.G., 2007. The decadal relationship between atmospheric heat source of winter and spring snow over Tibetan Plateau and rainfall in East China. Acta. Meteorol. Sin. 65, 946–958.